

Surface Morphology of Drying Latex Films: Multiple Ring Formation

Leonid Shmuylovich, Amy Q. Shen, and Howard A. Stone*

*Division of Engineering and Applied Sciences, Harvard University,
Cambridge, Massachusetts 02138*

Received September 27, 2001. In Final Form: February 11, 2002

When a drop of aqueous solution containing suspended particles dries, particles accumulate at the contact line. Often the contact line undergoes a sequence of pinning–depinning events with particles accumulating whenever the contact line is pinned. These processes lead to ring formation, the details of which are examined here. In particular, we provide detailed measurements of ring formation as a function of the drop radius and the size of the suspended particles, and we report measurements of the time dependence of the essentially stochastic pinning–depinning cycles of the contact line motion.

1. Introduction

Many studies have been performed on the formation of two-dimensional arrays by evaporation of a drop of liquid on a substrate.^{1–4} The solution is typically a suspension of latex or metal spheres, polymer, or protein in water. In these systems particles accumulate at the contact line and form ordered arrays. The formation of well-ordered two-dimensional arrays of particles has found use in materials science applications, including variants of lithography, where latex particles are deposited on a silicon substrate and used as an etching mask (e.g. ref 3, Chapter 13 and ref 5); also, two-dimensional arrays of protein can be used for many biological applications, including making sensors for immune cells.³ In addition to film formation and particle ordering, different groups have focused on how micron size particles are distributed after the drying process is complete;^{6–11} submonolayers of nanometer size particles have also been studied.⁴ For example, Deegan⁸ has reported on pattern formation in which particles are arranged in concentric rings within the drop. Deegan's observations had similarities to initial observations of such stripe patterns by Adachi et al.⁶ In this paper we study detailed features of these rings, which allows us to draw some conclusions regarding proposed models for this phenomenon.

It is well established that because the evaporation rate from a pinned drop is greatest at the edge (i.e., the stationary contact line), there is a flow of water toward the edge. This idea was used by Deegan et al.⁷ to explain

why rings of micron size particles form on the outside of coffee stains: when the contact line is pinned and evaporation occurs, particles flow toward it and become concentrated at the edge. A similar idea about the bulk flow of water in the drop due to evaporation was first put forward by Denkov et al.⁹ Their system did not have a contact line; instead, they put their drop inside a Teflon ring and studied the ordered, crystalline array of latex particles that formed due to an evaporatively driven convective flux toward the center of the experimental cell since this was where the evaporation rate was highest. In addition to the long-range convective flow, there are also (localized) lateral capillary forces that contribute to the final stages of particle aggregation and ordering.¹²

Adachi et al.⁶ observed that circular stripe patterns, or rings, formed inside the dried drops containing micron size particles and further noticed that the three-phase (water, air, glass) contact line exhibited stick–slip motion as the water evaporated. It is important to note that the motion of the contact line actually refers to the disappearance of water due to evaporation and not necessarily to the lateral (receding) physical movement of fluid in the neighborhood of the contact line. Adachi et al.⁶ suggested that the oscillatory, stick–slip motion of the contact line caused the formation of the stripe patterns (since particles accumulate at the contact line when it sticks), and they proposed a model for the stick–slip motion. Deegan further investigated pattern formation and showed that sometimes an isolated drying drop can form concentric ring patterns.⁸ Small (0.1 μm diameter) particles were observed to form concentric rings while larger (1 μm diameter) particles tended to form patterns without concentric rings.

We note that annular rings are also observed during the drying of small drops (0.1–1 μm diameter) containing nanoparticles.⁴ For these systems, it is argued that hole formation in the very thin films is responsible for the submonolayer annular rings. Hence, it appears that there is a mechanistic difference between the drying patterns formed with micron size particles and nanoparticles.

In this paper we report the results of experiments on concentric ring formation and contact line pinning/depinning. In particular, we show that concentric ring formation is possible for both 0.88 and 3.15 μm diameter particles, and the dynamics of ring formation is explored further. In section 2 we outline the experimental methods.

(1) Denkov, N. D.; Veleev, O. D.; Kralchevsky, P. A.; Ivanov, I. B.; Yoshimura, H.; Nagayama, K. *Nature (London)* **1993**, *361*, 7.

(2) Duskin, C. D.; Yoshimura, H.; Nagayama, K. *Chem. Rev. Lett.* **1993**, *204*, 5.

(3) Kralchevsky, P. A.; Nagayama, K. *Particles at Fluid Interfaces and Membranes*; Elsevier: Amsterdam, 2001.

(4) Ohara, P. C.; Gelbart, W. M. *Langmuir* **1998**, *14*, 3418.

(5) Karthaus, O.; Maruyama, N.; Cieren, X.; Shimomura, M.; Hashigawa, H.; Hashimoto, T. *Langmuir* **2000**, *16*, 15.

(6) Adachi, E.; Dimitriov, A. S.; Nagayama, K. *Langmuir* **1995**, *11*, 1057.

(7) Deegan, R. D.; Bakajin, O.; Dupont, T. F.; Huber, G.; Nagel, S. R.; Witten, T. A. *Phys. Rev. E* **2000**, *62*, 1.

(8) Deegan, R. D. *Phys. Rev. E* **2000**, *61*, 1.

(9) Denkov, N. D.; Veleev, O. D.; Kralchevsky, P. A.; Ivanov, I. B.; Yoshimura, H.; Nagayama, K. *Langmuir* **1992**, *8*, 3183.

(10) Deegan, R. D.; Bakajin, O.; Dupont, T. F.; Huber, G.; Nagel, S. R.; Witten, T. A. *Nature (London)* **1997**, *389*, 827.

(11) Cardoso, A. H.; Leite, C. A. P.; Zaniquelli, M. E. D.; Galembeck, F. *Colloids Surf. A* **1998**, *144*, 207.

(12) Kralchevsky, P. A.; Nagayama, K. *Langmuir* **1994**, *10*, 23.

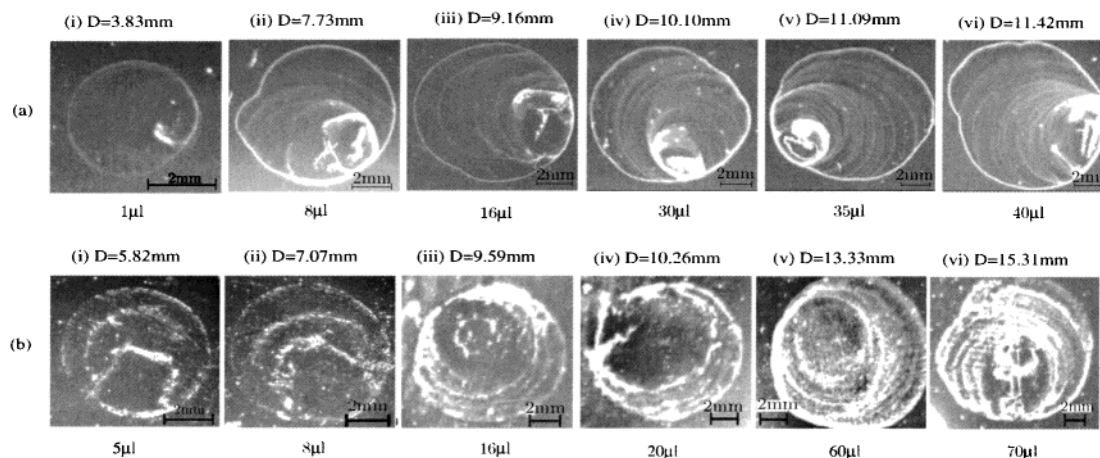


Figure 1. Multiple rings following the drying of drops of latex solution. The diameter D is given above the image of each drop. (a) $0.88\ \mu\text{m}$ diameter particles with varying drop volumes. The number of rings increases with drop volume (and therefore drop radius). All solutions were 0.008 wt %. (b) $3.15\ \mu\text{m}$ diameter particles with varying drop volumes. The concentric rings are not as pronounced as with the $0.88\ \mu\text{m}$ diameter particles, but as drop volume (and therefore drop radius) increases, the number of rings increases. All solutions were 0.01 wt %. Note that these images have been inverted for clarity; the originals show the particles as black and the background as white.

Section 3 summarizes the observations and the results of our experiments. Finally, we discuss how particle size may affect the way in which the contact line gets pinned. We also include observations of the local “self-healing” of defects during the two-dimensional ordering of a monolayer array of particles at the contact line, which represents some of the late stage dynamics of particle accumulation at the contact line.

2. Experimental Setup

Observations were made of drying latex solutions with bright-field microscopy. A surfactant-free monodisperse suspension with 8 wt % $0.88\ \mu\text{m}$ diameter polystyrene particles in water was purchased from Bangs Inc. We then made a suspension with weight percentage 0.008% and pH = 6 by diluting the original suspension with deionized water. A second surfactant-free suspension consisting of $3.15\ \mu\text{m}$ diameter particles, initially 10 wt %, was purchased from Duke Scientific. From this suspension we made a solution with weight fraction of 0.01% and pH = 6.

Drying films were made by placing a small droplet of solution on a 3×1 in. glass microscope slide, which was purchased from Corning and came in a precleaned condition. The drop diameters were varied between 1 and 15 mm. The concentration, volume, and evaporation rate were also varied for both solutions. In the experiments reported here evaporation took place under normal laboratory conditions. The results shown below were reproducible for experiments conducted on many different days, where ambient conditions (e.g., humidity, evaporation rate, and convective currents) may have varied, which demonstrates, at least qualitatively, the robustness of these observations.

Videos of the drying process were made with a CCD camera attached to a Leica light microscope. The effect of the light source from the microscope was assumed to be minimal since the droplet was uniformly illuminated, and so is not believed to contribute to the dynamics in the experiment. Image analysis was performed using frame-grabber software. In particular, we tracked the motion of the contact line during the evaporation process. We were able to examine the motion of the contact line on the scale of individual particles.

3. Results

We report results for the structure of the film during the drying process and for the surface morphology of the film after the drop is completely dry. To begin with, in Figure 1 we show the results of several experiments in which we observed film formation in dilute latex solutions. Figure 1a shows results for suspensions of $0.88\ \mu\text{m}$ diameter particles, where the concentration of the solution

was 0.008 wt % in each case. In the photographs shown the initial drop volume of latex solution was varied, and a scale bar is shown for each photograph. Changing the volume was a way to control the diameter of the drop and therefore the area covered by the drop. The particles show up as white while the glass slide is the dark background.

Shortly after placing the drop on the glass substrate, we observe the particles accumulating at the initial contact line. As evaporation occurs, the contact line moves (generally toward the center) and consequently multiple rings form. When a small volume was used, the drop covered only a small area of the substrate, and there was only one ring inside the drop. As the volume, and, therefore the diameter of the drop, increased, we observed more rings. Also, Figure 1a(ii–vi) shows that the highest concentration of particles is not found at the center of the drop. Instead, the highest concentration of particles is found closer to the edge. For example, in Figure 1a(v), the highest concentration of white is found closer to the left edge, which suggests that the right edge was not pinned as effectively as the left edge. Particles were pushed closer to the left edge as the contact line moved.

Figure 1b shows similar results for the $3.15\ \mu\text{m}$ diameter particles. It is important to note that the previous studies^{6,8} have not observed multiple ring formation for suspensions consisting of particles greater than $1\ \mu\text{m}$ in diameter, whereas Figure 1b shows that even $3.15\ \mu\text{m}$ particles can form multiple rings. Furthermore, for similar diameter drops, the results displayed in Figures 1a and 1b are very different. For example, Figure 1a(iv) and Figure 1b(iv) both had drop diameters of about 10 mm. However, the drop in Figure 1a, which had the smaller particles, clearly has more rings than the drop in Figure 1b. The same trend, with respect to the number of rings holds in Figure 1b as the one observed in Figure 1a, as the drop volume and diameter increase, the number of rings increases. We believe that the trends in Figure 1, i.e., the dependence of particle size and drop diameter on the formation of rings, have not been reported before. One reason that earlier studies^{6,8} may not have observed the connection between particle size, drop diameter, and ring formation is that they were limited to one drop size though particle sizes varied.

In Figure 2 we focus on the time dynamics of the contact line. In particular, we display a series of images during

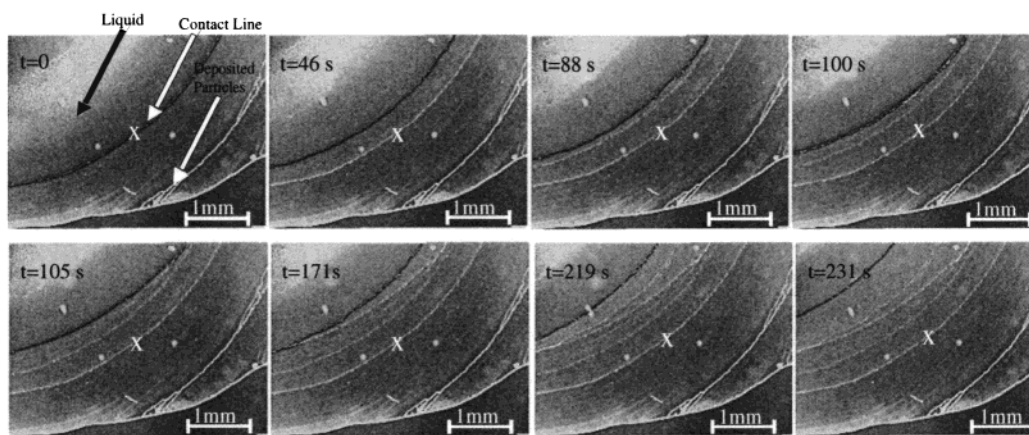


Figure 2. In this series of images the liquid drop is in the top left corner, and the deposited $0.88\ \mu\text{m}$ diameter particles are on the bottom right. The colors in the images were inverted for better resolution, so the current location of the contact line is the black line joining the liquid and solid, the gray corresponds to the glass slide, and white corresponds to deposited particles. The $t = 0$ location of the contact line is marked by a white "x" in all of the images and corresponds to the time of the first image. This "x" is always in the same location relative to the drop. In each image the contact line is pinned. Notice that a ring deposit was left behind wherever the contact line was pinned.

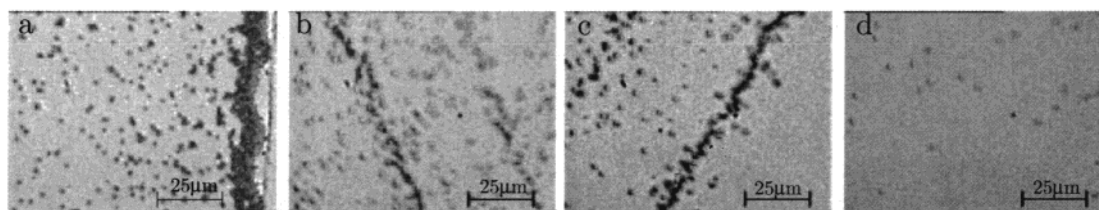


Figure 3. A series of $63\times$ magnification photographs of a completely dry drop consisting of $0.88\ \mu\text{m}$ diameter polystyrene particles. (a) The right part of this image is the edge of the drop. The gray background is the glass slide, and the particles have aggregated at the edge. (b, c) Photograph of the ring deposit which is seen to be typically only 1–2 particles in width. (d) This is an area of the dry drop where there is no ring deposit and only a few scattered particles.

evaporation of a 18 mm diameter drop consisting of $0.88\ \mu\text{m}$ diameter particles. The images show the ring deposits, which serve as a record of the places where the contact line was pinned during the drying process; the particles appear as white and accumulate whenever the contact line is pinned. The current location of the contact line in each image is represented by the black line. A white "x" marks the location where the first contact line in this sequence was pinned, and this initial location is indicated in each image.

In the photograph labeled $t = 0$, the contact line is not in motion, but rather it is pinned to the glass substrate. A few seconds later it gets "depinning" and begins to move. However, at $t = 46\ \text{s}$, the contact line gets pinned again. It stays pinned for several seconds, and then once again starts moving, only to be stopped at $t = 88\ \text{s}$. This cycle of pinning and depinning continues throughout the drying process. It is also clear from examining the final photograph at $t = 231\ \text{s}$ that the white lines, representing areas where the particles are highly concentrated, are found in exactly the same positions where the contact line was pinned in the previous photographs.

Between the photographs labeled $t = 105\ \text{s}$ and $t = 171\ \text{s}$ in Figure 2 we can see that it is possible for part of the contact line to stay pinned while another part moves. The left-most part of the contact line in these pictures remains stationary while the rest of the line moves. The resulting deposit therefore seems to branch. This suggests that not all parts of the contact line are pinned equally well to the glass, as was also indicated in some of the results shown in Figure 1. We have not been able to quantify this further, but it is evidence of the rich and complicated nature of the contact line motion during drying.

Figure 3 is a close-up view of the ring deposits in a drop consisting of $0.88\ \mu\text{m}$ diameter particles. It is clear from this series of photographs that, perhaps surprisingly, typical interior ring deposits are only a few particles wide. This observation is quite different from particle accumulation at the initial edge of the drop (Figure 3a), which is anywhere from 10 to 20 particles wide.

In Figure 4 we quantify some of our results about the stick-slip motion of the contact line. We plot the distance that the contact line traverses between successive starts and stops vs time (e.g., as shown in Figure 2). We also show the distribution of distances traversed by the contact line between starts and stops. In two separate experiments the average distances traversed by the contact line for a drop consisting of $0.88\ \mu\text{m}$ diameter particles were 583 and 717 μm . The average time that the contact line was moving in the first run was 17 s while the average time that the contact line was pinned was 50 s. In general, based on many other experiments, the typical time that the contact line was pinned is longer than the time that the contact line was moving. For drops consisting of 3.15 μm particles we have similar results, one of which is displayed in Figure 4b. The average distances traversed by the contact line in two different runs were 766 and 853 μm . With these larger particles we also observed that the time the contact line was pinned was usually longer than the time that it was moving. However, the difference between these times was not as large as with the smaller particles. This is not that surprising given that, for the same volume fraction, the distance that the contact line moves in a suspension with bigger particles is greater than the distance it moves in a suspension of smaller particles (see discussion below).

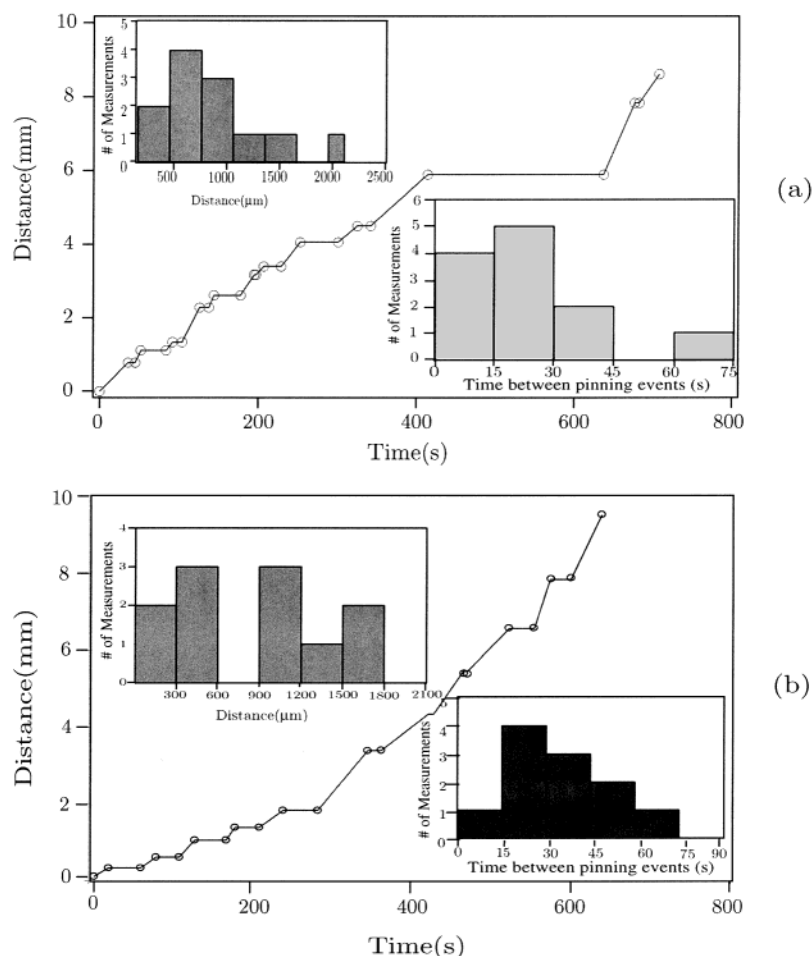


Figure 4. (a) Stick-slip motion of the contact line with $0.88 \mu\text{m}$ diameter particles. The vertical axis is the distance (measured from near the edge of the drop) that the contact line moved. A bar graph of the distribution of the distances traversed by the contact line between successive “sticking events” is also given. The average distance traversed by the contact line is $717 \mu\text{m}$. In addition, a bar graph of the distribution of times that the contact line was moving is given. (b) Similar graphs for $3.15 \mu\text{m}$ particles. The average distance traversed by the contact line is $853 \mu\text{m}$.

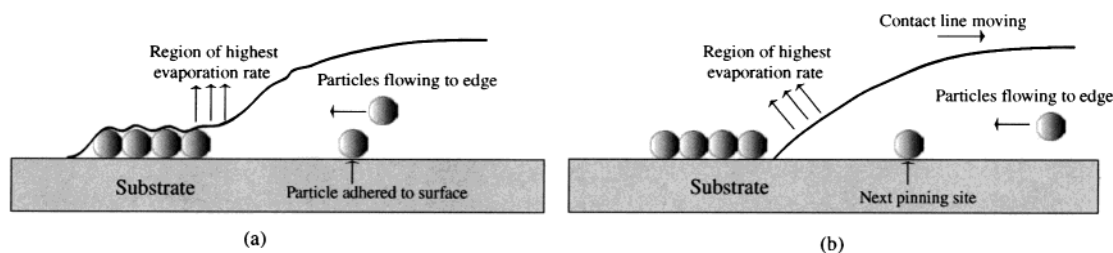


Figure 5. (a) A schematic for a pinned contact line. Evaporating water at the contact line induces a flow of particles toward the edge. However, some particles are pinned to the substrate. (b) Once the contact line “slips”, it keeps moving until it runs into a fixed particle, at which point it may become pinned again.

4. Discussion

We have reported on several dynamical features associated with drying dilute latex solutions. Because of the higher evaporation rates near the edge of a drying drop, the location of the three-phase contact line moves.¹⁰ In Figure 4 we showed that the distance that the contact line traverses and the time between pinning, or sticking, events have a rather broad distribution. At least in our experiments, the motion of the contact line is not a simple sinusoidal response as envisioned in the model for stick-slip motion proposed by Adachi et al.⁶

Although there is a flux of particles toward the contact line due to an evaporatively driven convective flow, the particles that pin the contact line do not flow toward the

contact line, but instead are pinned to the substrate (see Figure 5). For a given volume fraction ϕ , the probability of finding a particle in a given volume is proportional to ϕ . Since we expect a random distribution of particles, the average distance between two particles is proportional to $a\phi^{-1/3}$, where a is the particle radius. This represents the average distance that the contact line must move once it becomes depinned until it reaches the next fixed particle and therefore gets pinned again. For fixed ϕ , as a increases, the distance that the contact line moves between pinned sites is expected to increase. Also, as the evaporation rate is not changing significantly, it takes longer for the contact line to move between pinned and depinned states. These explanations are consistent with the experimental observations (Figure 4).

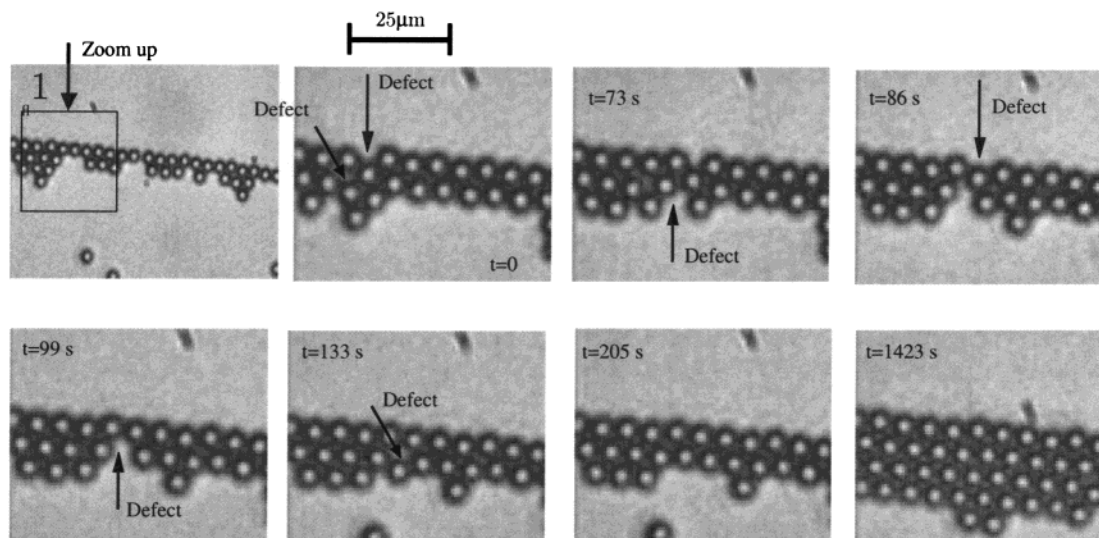


Figure 6. Self-healing of the crystalline structure formed from $3.15\ \mu\text{m}$ diameter particles. All of the images focus on the region shown in the photograph labeled 1. The image labeled $t = 0$ does not represent the initial time that drying began, but rather is the initial time of this sequence of photographs. The arrows point to defects in the structure. As the solution dries, the latex particles are sometimes not packed in a perfect hexagonal structure. As the drying process continues, these defects heal and an ordered structure is formed.

This view of contact line pinning and depinning is essentially stochastic and contrasts with the detailed physical model proposed by Adachi et al.⁶ Furthermore, a model proposed by Iliev¹³ for a pure water droplet showed that the hysteresis of the contact angle introduces stick-slip motion of the contact line. However, under constant evaporation conditions, the predicted stick-slip motion from such a model is (nearly) periodic. The irregularity of the contact line motion that we have observed (Figure 4) does not agree qualitatively with these two deterministic models. A generalization of Iliev's model considering the presence of particles may account for some of our observations, but this is beyond our present study.

As a final aspect of the dynamical events near the contact line associated with evaporation of dilute suspensions, we illustrate some features on the scale of individual particles. As mentioned earlier, one of the primary interests in studying the drying of latex suspensions is their ability to form a two-dimensional crystalline monolayer of closely packed particles. In Figure 6 we show how the (hexagonal) crystalline structure that is formed from the packing of latex particles can "self-heal" defects. These photographs show $3.15\ \mu\text{m}$ diameter particles packing at the edge of a drop. All of the photographs focus on the area near the edge indicated by the box in the first picture. "Defects" in the packing may be observed where "defects" refers to places where the particles are not perfectly packed. At $t = 0$ there are some defects in the upper left portion of the film, while at $t = 73\ \text{s}$ some of the defects

have disappeared. The particles physically rearrange themselves to fit into a more ordered configuration, but there are still defects at $t = 73\ \text{s}$. At $t = 133\ \text{s}$ we see that an oncoming particle has not fit itself perfectly in the lattice of particles. Later, at $t = 205\ \text{s}$, however, a particle filled in the defect without having been hit by any oncoming latex particles. Therefore, it is apparent that it was pushed in place by capillary forces associated with the (drying) film between the particles.⁹ Finally, at $t = 1423\ \text{s}$ we observe a well-ordered array.

In conclusion, we presented experimental results on multiple ring formation in an evaporating suspension droplet. The rings formed both for 0.88 and $3.15\ \mu\text{m}$ diameter particles (the latter having not been observed previously). Also, we studied the influence of changing the droplet diameter. Finally, we presented quantitative results illustrating that the pinning/depinning motion of the contact line was essentially stochastic.

Acknowledgment. We thank the Harvard MRSEC and the NSF for funding this work through Grant DMR-9809363 and PPG Industries for partial support. Also, we thank Tony Dinsmore, Bob Graham, Gareth McKinley, Nicolas Tapis, Shang Tee, Megan Valentine, and David Weitz for helping with the experiments, with data acquisition, and for many valuable suggestions. We thank an anonymous referee for pointing us to the paper by Iliev.¹³

(13) Iliev, S. D. *J. Colloid Interface Sci.* **1999**, *213*, 1.